A comprehensive in vitro and in vivo study of ZnO nanoparticles toxicity

Article · May 2013

DOI: 10.1039/C3TB20251H

6 authors, including:

Nirmalya Tripathy
University of Washington Seattle
59 PUBLICATIONS **1,051** CITATIONS
SEE PROFILE

Kitae Ha
Pusan National University
112 PUBLICATIONS **861** CITATIONS
SEE PROFILE

Han-Sol Jeong
Pusan National University
27 PUBLICATIONS **378** CITATIONS
SEE PROFILE

Yoon-Bong Hahn
Chonbuk National University
348 PUBLICATIONS **7,665** CITATIONS
SEE PROFILE

Journal of Materials Chemistry B

RSC Publishing

PAPER

A comprehensive *in vitro* and *in vivo* study of ZnO nanoparticles toxicity†

Cite this: *J. Mater. Chem. B*, 2013, **1**, 2985

Tae-Keun Hong,‡[a] Nirmalya Tripathy,‡[b] Hyun-Jin Son,[c] Ki-Tae Ha,[a] Han-Sol Jeong*[a] and Yoon-Bong Hahn*[b]

Nowadays, the exploration of zinc oxide nanoparticles (ZnO NPs) based products is booming in the various directions of bio-nanomedicine and other consumer products, but the comprehensive toxicological impact posed by ZnO NPs still remains unclear. The present study systematically investigates and correlates the toxicity evaluation of ZnO NPs in RAW 264.7 murine macrophages (*in vitro*) and male ICR mice (*in vivo*) by two different administration routes, *i.e.* g.i. and i.p. at different doses. The *in vitro* studies showed a slight rise in intracellular reactive oxygen species level (ROS), NF-κB transcription factor expression (TF) and NPs uptake at higher dose, indicating the non-toxic nature of ZnO NPs below 100 μg mL^{-1} doses. The *in vivo* results demonstrate a slight gain in body weight (BW), reduction in the organ weight, mild to severe pathological alteration in the organs depending upon NP dosage and mode of administration routes. The histopathological investigation suggests that the liver, kidney, lung, spleen, and pancreas may be the target organs for ZnO NPs according to the administration routes. Serum biochemistry assay shows an elevation in the GPT and ALP level, suggesting liver dysfunction. To our knowledge, this is the first study to report the toxic effects of ZnO NPs through i.p. administration. Further, the present work will offer a deeper understanding regarding the toxicology and *in vivo* behaviours of ZnO NPs in mice depending upon the various administration routes.

Received 20th February 2013
Accepted 2nd April 2013

DOI: 10.1039/c3tb20251h

www.rsc.org/MaterialsB

1 Introduction

The integration of biomedicine and nanotechnology has presented various advances in medical care where nanomaterials serve as biological mimetics, "nanomachines", laboratory diagnostics, shape–memory polymers as molecular switches, biomaterials for tissue engineering, nanoscale devices for drug release, and near real-time biosensors.[1–6] Because of their signature features, nanomaterials tend to interact with the cellular and subcellular structures more closely, resulting in a variety of toxicological end points.[7,8] ZnO NPs, a smart and versatile nanomaterial, have revolutionized many industries including pharmaceutics, cosmetics, paints, dietary supplements in humans and livestock, food additives and so on.[9–11] Importantly, ZnO NPs have gained immense interest in nanomedicine and biomedical applications owing to their high stability, low cost, inherent photoluminescence properties and wide band–gap semiconductor properties advantageous for biomolecule sensing, photo-catalytic systems and promotion of ROS.[12,13] Various external applications such as ointments, lotions, sunscreens, facial creams *etc.* also rely on the unique characteristics of ZnO like the ability to absorb ultraviolet A and B radiation, optical transparency and antibacterial properties.[14–16] Moreover, ZnO NPs show promise in modulating allergic reactions *via* inhibition of mast cell degranulation.[17] Such rapid and huge usage of these nanomaterials increases their likelihood to come into contact with the ecosystem. However, the available biological information on the toxicological impact posed by these materials is still incomplete, although their production and use in everyday products is booming.

The FDA considers ZnO as a "GRAS" (generally recognized as safe) substance. However, the GRAS designation most commonly refers to materials in the micron to larger size range. When reduced to the nano phase, these substances can develop new actions of toxicity.[18] Additionally, the SCCNFP (Scientific Committee on Cosmetic Products and Non-Food Products) have

[a]*School of Korean Medicine, Division of Applied Medicine, Pusan National University, 3-3 Beomeo-ri, Yangsan-si 626-870, Korea. E-mail: jhsol33@pusan.ac.kr*

[b]*Dept. of BIN Fusion Technology, School of Semiconductor and Chemical Engineering, Chonbuk National University, 567 Baekje-daero, Deokjin-gu, Jeonju 561-756, Korea. E-mail: ybhahn@chonbuk.ac.kr*

[c]*Dept. of Pathology, Eulji University School of Medicine, 143-5 Yongdu-dong, Jung-gu, Daejeon 301-746, Korea*

† Electronic supplementary information (ESI) available: Supplementary Fig. 1 shows the TEM images of (A) bare ZnO NPs, (B) aminated ZnO NPs showing a thin film coated on the ZnO surfaces, and (C) the surface charges of the bare and aminated ZnO NPs in aqueous solution at different pH measured by zeta potentiometer. Supplementary Fig. 2 shows the cellular uptake behavior of ZnO NPs. Supplementary Fig.3 shows the gross observation of mice after intraperitoneal administration of 100 μg mL^{-1} ZnO nanoparticles. See DOI: 10.1039/c3tb20251h

‡ TKH and NT contributed equally to this work.

reported that the LD_{50} of normal ZnO for rats is more than 5 g kg^{-1} BW and ZnO are non-toxic chemicals (showed by a single oral ingestion). However, the final opinion of the SCCNFP states that an appropriate safety dossier on micro-sized ZnO including possible pathways of cutaneous penetration and systemic exposure is still required.[19] To date, a huge number of studies were reported presenting insights of engineered nano-ZnO cytotoxicity, but most of these studies investigate the cytotoxic behaviour of nano-ZnO either in *in vitro* or *in vivo*. Previously reported *in vitro* toxicological data include the cytotoxic behaviour of ZnO NPs in different cell lines such as in RAW 264.7, BEAS-2B, human monocyte macrophages, and also in cancerous T cells.[20–23] A few *in vivo* studies have indicated that the liver, heart, spleen, pancreas and bone all appear to be target sites of ZnO NPs in mice, and inhalation of these particles in rats produces potent yet reversible pulmonary inflammation.[24,25] Moreover, the pharmacokinetics and toxicology of a drug or biomaterial are closely related with its administration routes. Although a substantial understanding have been achieved by the researchers regarding the *in vitro* and *in vivo* toxicology behaviours of ZnO NPs, the fate of ZnO NPs in animals after g.i. and i.p. administration, which are the two major drug administration routes, is still unclear.

This study was designed to systematically evaluate and correlate the toxic responses induced by a common stock of ZnO NPs prepared *via* low temperature aqueous route, in both *in vitro* and *in vivo* for its better risk assessment in humans. These basics will further assist in devising means for mitigating its risks and maximizing benefits. Firstly, the toxic evaluation including ROS generation, oxidative stress, NF-κB TF expression, pro-inflammatory responses and particle uptake behaviour of ZnO NPs was carried out in RAW 264.7 murine macrophages (*in vitro*). Next, the *in vivo* behaviour was observed over a period of 14 days in male ICR mice according to the guidelines of the single dose toxicity study presented by the Korean National Institute of Food and Drug Safety Evaluation which suggested 14 days' observation periods to examine the single dose toxicity. This includes determination of serum biochemical level, organ indices and histopathological changes in detail, after g.i. and i.p. administration.

2 Experimental

2.1 Materials

Zinc acetate dihydrate ($Zn(O_2CCH_3)_2(H_2O)_2$), hexamethylenetetramine (HMTA, 99%), lithium hydroxide (LiOH), fluorescein isothiocyanate (FITC) and phosphate-buffered saline (PBS; pH 7.4) were purchased from Sigma–Aldrich. Biological reagents used for cell culture experiments such as Dulbecco's modified Eagle's medium (DMEM), 2′,7′-dichlorfluorescein-diacetate (DCFH-DA), G418 (600 μg mL^{-1}), trizol reagent and lipofectamine were purchased from Invitrogen (Carlsbad, CA, USA); penicillin/streptomycin (with 10 000 units penicillin and 10 mg of streptomycin per mL), fetal bovine serum (FBS) and L-glutamine (200 mM) were purchased from Hyclone (Logan, UT, USA); pEGFPLuc came from BD Biosciences, San Jose, CA, USA, and M-MLV reverse transcriptase and Bright-Glo™ Luciferase Assay System came from Promega, Madison, WI, USA. The kit used for cytotoxicity test was a proliferation kit II (XTT; sodium 2,3-bis (2-methoxy-4-nitro-5-sulfophenyl)-5-[(phenylamino)-carbonyl]-2*H*-tetrazolium) and was purchased from Boerhringer Mannheim (Mannheim, Germany).

2.2 ZnO NPs synthesis

First, ZnO NPs were synthesized by low temperature solution route using Zinc acetate dihydrate, HMTA, and LiOH followed by washing and drying in air as previously described.[26] For the aminated ZnO NPs, 0.1 g of ZnO NPs was dispersed in ethanol solution (50 mL), to which ammonia solution (1.5 mL, 28 wt%), TEOS (15 μL) and APTES (60 μL) were added and stirred for 3 h. The obtained products were then washed with ethanol and air dried at room temperature. For uptake studies, FITC-labelled ZnO (FITC–ZnO) NPs were synthesized by functionalizing the NPs surface with amino groups using APTES/TEOS.[27] As it is known that the isothiocyanate group of FITC easily interacts with amine groups, to 20 mL NPs solution, 50 μL FITC (1 mg mL^{-1} in DMSO) were added and stirred for 2 h. The FITC–ZnO NPs were washed to remove non-bound FITC and air dried. The structural characterization, crystallinity and surface charge of NPs were studied by transmission electron microscopy (TEM) and X-ray diffraction (XRD) in the range of 20–70° with 8° per min scanning speed on a zeta potentiometer (Zetasizer Nano ZS system, Malvern Instruments, Malvern, Worcestershire, UK). The hydrodynamic diameter of NPs in water was measured with a dynamic light scattering (DLS) particle size analyzer (ELSZ-2, Otsuka Electronics Co., Ltd., Osaka, Japan). The optical properties are examined by room-temperature photoluminescence (PL) spectroscopy with He–Cd (325 nm) laser lines as the exciton source.

2.3 Cell culture

The RAW 264.7 murine macrophages were obtained from ATCC (American Type Culture Collection, Rockville, MD, USA) and cultured in DMEM containing L-glutamine (200 mg L^{-1}) supplemented with 10% (*v*/*v*) heat-inactivated fetal bovine serum (FBS), 100 U per mL penicillin and 100 μg mL^{-1} streptomycin and maintained in a humidified incubator at 37 °C and 5% CO_2 prior to the experiments. Additionally, the ZnO NPs colloidal suspension was carefully sonicated before each experiment in order to minimize aggregation effects.

2.4 Assessment of cell viability and ROS generation

Cell viability was assessed by the XTT assay. Briefly, cells (10^4 per well) in 100 μL DMEM with 10% FBS culture medium were plated in 96-well plate and incubated in 5% CO_2 at 37 °C. After 24 h, the medium was replaced with 100 μL of new medium containing 0.1, 1, 10, and 100 μg mL^{-1} ZnO NPs and incubated in 5% CO_2 at 37 °C for 24 h. Then, 50 μL of XTT labelling mixture was added, incubated for 4 h and the absorbance was measured using an ELISA reader (VERSAmax, Molecular Devices) at a test wavelength of 490 nm.

Intracellular ROS generation of RAW 264.7 murine macrophages was determined using a ROS fluorescent probe,

DCFH-DA. Briefly, after ZnO NPs administration, cells were treated with 10 μM DCFH-DA in cultured medium and incubated at 37 °C for 20 min. After incubation, the cells were washed with PBS and the fluorescence was measured using a 1420 multilabel counter (Victor™; Perkin-Elmer Life Sciences, Wallac Oy) with an excitation wavelength of 485 nm long pass, and an emitter band pass of 535 nm.

2.5 Pro-inflammatory cytokine mRNA analysis

After incubation of cells with 1 μg mL^{-1} ZnO NPs, the total RNA was isolated by using the Trizol reagent according to the manufacturer's instructions. After the concentration of RNA was determined by spectrophotometer, 1 μg of RNAs was reverse-transcribed by M-MLV reverse transcriptase and amplified by PCR with specific primers. Finally the amplified cDNA products were separated on 1.5% agarose gel by electrophoresis and TNF-α, IL-1β and MCP-1 cytokine level was monitored.

2.6 Reporter constructs, reporter cell line, and luciferase assay

To measure NF-κB transcriptional activity, an NF-κB reporter construct was created and transfected into RAW 264.7 cells. The reporter construct harbours four tandem copies of 36-base enhancer from 5′ HIV-long terminal repeat (containing two NF-κB binding site, GGGACTFTTTCC) placed upstream of the HSV minimal thymidine kinase promoter, which were cloned into pEGFPLuc. Then the reporter construct was introduced into RAW 264.7 cells by transfection using lipofectamine and the transfected cells were selected under G418 (600 μg mL^{-1}). Candidate cell lines harbouring the NF-κB reporter construct were tested for luciferase activity. These cells (10^5 per well) in 100 μL DMEM culture medium were then plated in a 12-well plate and incubated in 5% CO_2 at 37 °C. After 24 h, the medium was replaced with new medium containing 1, 10 and 100 μg mL^{-1} ZnO NPs and 1 μg mL^{-1} lipopolysaccharide (LPS; positive control) and incubated in 5% CO_2 at 37 °C for 4 h and 16 h. Then, 150 μL of supernatant was removed from all wells and 100 μL per well Glo® Lysis Buffer for 5 min, 100 μL Bright-Glo® Luciferase Assay System reagent was added. The luminescence was measured using Tecan Infinite F500 multimode plate reader.

2.7 Cellular uptake

Cells (10^6 per well) in 100 μL DMEM culture medium were plated in 96-well plate and incubated in 5% CO_2 at 37 °C. After 24 h, the medium was replaced with 100 μL of new medium containing 1, 10 and 100 μg mL^{-1} FITC–ZnO NPs and incubated in 5% CO_2 at 37 °C for 1, 2 and 4 h. After incubation, the cells were washed with PBS 3 times. Finally, the cells were re-suspended in PBS followed by flow cytometry analysis (FCM) (FACS Canto II Analyzer, BD Biosciences, San Jose, CA, USA).

2.8 Animals and treatment

Healthy male ICR mice, weighing about 35 g (9 weeks old) were purchased from Samtaco Bio Korea, Ltd. (Osan, Korea). The animal protocol used in this study has been reviewed by the Pusan National University-Institutional Animal Care and Use Committee (PNU-IACUC) on their ethical procedures and scientific care, and it has been approved (Approval Number PNU-2012-0186). The animals were housed in clean polypropylene cages and maintained in an air-conditioned animal house at 20 ± 2 °C, 50–70% relative humidity and 12 h light–dark cycle. They were provided with a commercial rat pellet diet and water. After one week acclimation, the mice were randomly divided into seven groups (six in each group), comprising one control group and six experimental groups. Prior to the experiment, the ZnO NPs were suspended in PBS (pH 7.14) and ultrasonicated for 10 min. For concentration-dependent toxicological experiments, the mode of administration was selected to be g.i. and i.p. Then the mice were administered with 1, 10 and 100 mg kg^{-1} BW ZnO NPs, allotted as G1, G2, G3 and I1, I2, I3 respectively, for g.i. and i.p. administration. After daily administration, the mice were weighed as well as observed for behavioural alterations, and sacrificed after injection of ZnO NPs for 14 days.

2.9 Biochemical assay of serum

To determine the serum biochemical levels including the alanine aminotransferase (ALT/GPT), creatinine (CRE), blood urea nitrogen (BUN), and alkaline phosphatase (ALP), the whole blood was centrifuged at 3000 rpm for 15 min and assayed by an automatic biochemical analyzer.

2.10 Histopathological observation

A small piece of heart, liver, kidney, spleen, lung, pancreas, stomach, and brain was fixed by 10% formalin and then embedded into paraffin, sectioned for 5–6 mm thick, and mounted on the glass microscope slides using standard histopathological techniques. The sections were stained with hematoxylineosin and examined by light microscopy.

2.11 Statistical analysis

All data are expressed as the means ± standard error (SEM) of at least three independent experiments. For comparison among groups, one-way analysis of variance (ANOVA) test were used (with the assistance of Graph pad Software, Inc., San Diego, CA).

3 Results and discussion

3.1 Characterization of ZnO NPs

Fig. 1 shows the TEM images for (A) bare ZnO and (B) FITC–ZnO NPs synthesized by low temperature solution route along with the DLS measured particle size distributions presented in the respective inserts. From the image (A), the as-synthesized ZnO NPs were found to be well-dispersed and spherically shaped with a diameter varying in the range of ~20 ± 5 nm. The TEM image of FITC–ZnO NPs shows an increase in the NP size which is attributed to the size of the FITC molecule, *i.e.* ~1.2 nm.[28] (The confirmation of ZnO NPs surface functionalization with amine group is shown in ESI Fig. S1†). This also suggests that FITC may exist as a single molecule or small clusters on the ZnO matrix. Additionally, the average hydrodynamic sizes of the bare

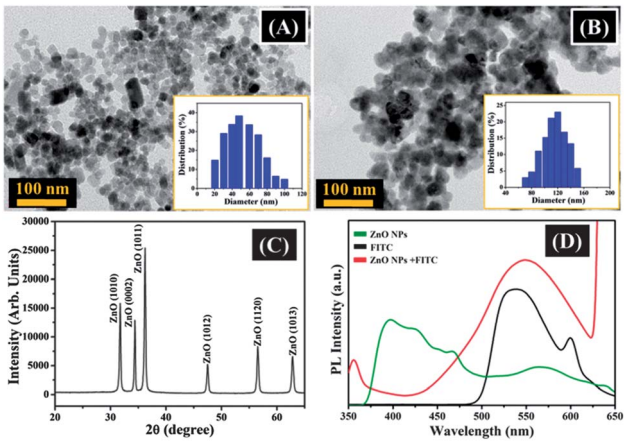

Fig. 1 Typical TEM images with respective DLS measured particle size distribution in the inset for (A) bare ZnO and (B) FITC–ZnO NPs; (C) XRD pattern of ZnO NPs, and (D) room temperature PL spectra of ZnO NPs, FTIC and FITC–ZnO NPs.

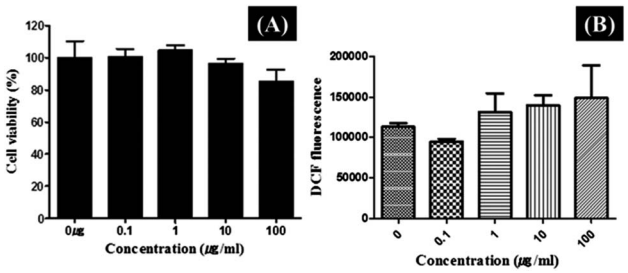

Fig. 2 Effect of ZnO NPs on (A) cell viability and (B) intracellular ROS production. The RAW 264.7 murine macrophages were treated with 0.1, 1, 10 and 100 μg mL^{-1} ZnO NPs for 24 and 1 h prior to the XTT assays and ROS assessment assay including addition of DCFH-DA for 30 min followed by FACS analysis. No significant adverse effect was observed for ZnO. All the values are represented as mean ± S.D. of three individual experiments.

ZnO and FITC–ZnO NPs determined by DLS particle size analyzer were 37 nm and 120 nm, respectively. The obtained hydrodynamic diameters are larger than in the TEM images due to the aggregation propensity of the particles. Moreover, the polydispersity index (PDI) for the bare and FITC–ZnO NPs are found to be 0.234 and 0.171, respectively. The purity and crystallinity of the as-synthesized ZnO NPs were analyzed by XRD which shows all the peaks belong to the hexagonal wurtzite phase (JCPDS Card no. 36-1451), shown in Fig. 1C. Fig. 1D shows the optical characteristics of the bare ZnO NPs, FITC–ZnO NPs and FITC molecules analyzed by room temperature PL spectra. The pure FITC and the bare ZnO NPs showed emission peaks at 537 and 376 nm, respectively.[29,30] Compared to the FITC molecules and the ZnO NPs, a stronger emission peak at longer wavelength (552 nm) was obtained for the FITC–ZnO NPs.[31] This strong emission enhancement and the red shift in the composites are associated with the interaction between the ZnO matrix and FITC.

3.2 Cell toxicity and ROS generation

ZnO NPs, at very high concentrations, particularly those in the smaller size range of 4–20 nm, were observed to cause harmful effects to normal body cells.[32] Keeping in mind the above fact, the effect of ~20 ± 5 nm ZnO NPs in RAW 264.7 murine macrophages was assessed by determining the mitochondria dehydrogenase activity with XTT assay. The XTT assay was performed after treating RAW 264.7 murine macrophages with 0.1, 1, 10 and 100 μg mL^{-1} ZnO NPs for 24 h, as shown in Fig. 2A.

Up to a concentration of 100 μg mL^{-1}, ZnO NPs did not produce any significant cytotoxicity, albeit a slight reduction in cell viability was observed as the concentration reached 100 μg mL^{-1}. High intracellular ROS levels and oxidative assault have been cited as important factors for cellular damage induced by various nanomaterials including quantum dots and nano-metal oxides although a few reports address the capability of ZnO NPs to induce ROS in normal/non-transformed human cells.[33] To investigate the ZnO NPs potential to induce ROS generation in RAW 264.7 murine macrophages, a fluorescent indicator, *i.e.* DCFH-DA dye, was employed followed by FACS analysis. The DCFH-DA passively enters the cell where it reacts with ROS to form the highly fluorescent compound dichlorofluorescein (DCF). Fig. 2B shows the ROS level in RAW 264.7 murine macrophages after exposure to 0.1, 1, 10 and 100 μg mL^{-1} ZnO NPs for 1 h. The induction of intracellular ROS level was found to be dose-dependent with a very little increment in the fluorescence level. Furthermore, the ZnO NPs induced ROS generation results are consistent with their effect on cell viability.

3.3 Pro-inflammatory cytokine mRNA expression

Several published studies have emphasized the ability of nanomaterials to induce cytokine production, which are soluble biological protein messengers regulating the immune system.[34] Gojova *et al.* have shown that ZnO NPs increase IL-8 and MCP-1 cytokine mRNA expression in human aortic endothelial cells, although no information was provided regarding changes in corresponding protein levels.[35] Also, studies conducted in immortalized primary alveolar macrophages, rodent lung epithelial cells and alveolar macrophage cell lines showed that the ZnO NPs was unable to induce TNF-α even at high concentrations.[36] Similarly, expression of IL-1β and chemokine CXCL9 induced by 20 nm ZnO NPs in murine bone marrow-derived dendritic cells and RAW264.7 murine macrophages were observed.[37] To evaluate whether ZnO NPs elicit an acute immunological response, the secretions of pro-inflammatory cytokines TNF-α and IL-1β together with anti-inflammatory cytokines MCP-1 were analyzed as they represent critical pathways involved in the inflammatory response and differentiation processes, as shown in Fig. 3. In the case of both TNF-α and MCP-1 secretions, no change was observed in the treated groups compared to the negative control. Interestingly, an appreciable amount of IL-1β production was recorded at a low concentration of ZnO NPs. The ZnO NPs inability to induce TNF-α, MCP-1 secretions and ability to induce at least some key components of inflammation, *i.e.* IL-1β production in our studies, is consistent with the above reports. It is quite interesting to point out that inhalation of ultrafine ZnO particles in occupational settings

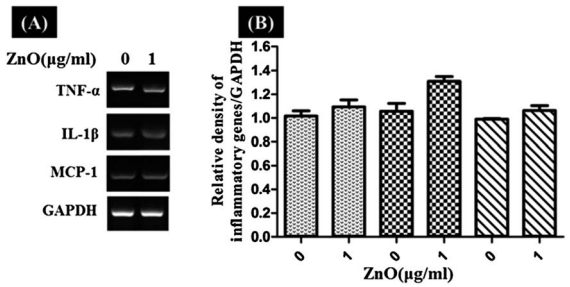

Fig. 3 Effect of ZnO NPs on pro-inflammatory cytokine mRNA expression. (A) Total RNA was extracted, and the expression of pro-inflammatory genes, including TNF-α, IL-1β, MCP-1, was analyzed by semi-quantitative RT-PCR. (B) Relative expression of each gene against GAPDH was determined by densitometric analysis of each band.

can increase the expression of these cytokines, symptomatically recognized as metal fume fever in welders (*e.g.*, chills, fever, cough, myalgias, fatigue and leukocytosis).[33]

3.4 NF-κB TF expression

The potential of ZnO NPs to induce pro-inflammatory cytokine expression is consistent with the recognized relationship between oxidative stress and inflammation, partially mediated by induction of NF-κB TF.[38] Hence, the NF-κB TF expression was analyzed by luciferase assay as described in Fig. 4. The luciferase reporter contains a *cis*-acting DNA binding element, recognized by a specific TF and binding at this site expresses luciferase enzyme. The resulting chemical reaction will emit light directly proportional to the amount of expressed enzyme and thus the binding activity of the targeted TF. Lower concentrations of ZnO NPs (1 and 10 μg mL^{-1}) yield a decreased luciferase activity whereas a mild increased luciferase activity was monitored at a high concentration of ZnO NPs (*i.e.* 100 μg mL^{-1}). All these results imply a slight increase in the NF-κB activity which is in correlation with intracellular ROS production and cell viability outcomes (Fig. 2A and B).

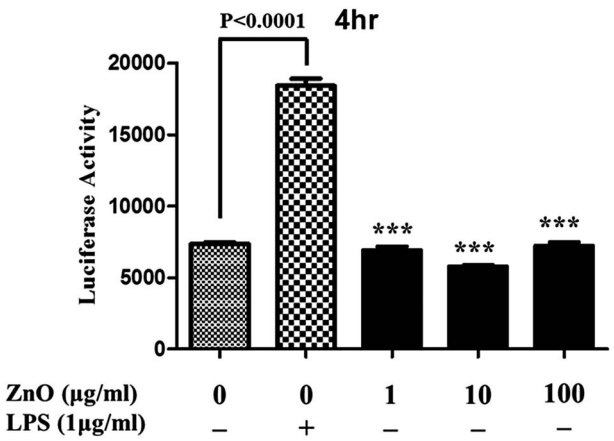

Fig. 4 Effect of ZnO NPs on the expression of NF-κB transcription factor. The RAW 264.7 murine macrophages were treated with 1, 10 and 100 μg mL^{-1} ZnO NPs and 1 μg mL^{-1} LPS for 4 and 16 hours, followed by luciferase assay. ***P < 0.0001, statistically significant difference compared to the untreated (1st column).

3.5 Uptake behaviour

Fig. 5 shows the permeation ability and cellular uptake behaviour of ZnO NPs through the cell membrane, examined after NPs followed by FACS analysis. The detailed FACS results are shown in the ESI Fig. S2.† The cells incubated while treating the RAW 264.7 murine macrophages with FITC–ZnO in the absence of particles served as negative control. At lower concentrations of ZnO NPs (1 and 10 μg mL^{-1}), an almost negligible alteration in the uptake behaviour of the treated cells was observed, whereas a little raise in ZnO NPs uptake was noticed at 100 μg mL^{-1} ZnO NPs. This further suggests that particle uptake is associated with intracellular ROS production and cell viability outcomes (Fig. 2A and B). Compared to the cellular uptake behaviour, ZnO NPs fail to induce high levels of NF-κB TF expression in RAW 264.7 murine macrophages as only IL-1β (known inducer of NF-κB TF expression) production was observed in Fig. 3. This suggests very little involvement of NF-κB TF expression in the toxicity of ZnO NPs in RAW 264.7 murine macrophages. Notably, ZnO NPs concentration reaches a saturation point in the treated cells at 2 h, after which an eventual reduction in the uptake behaviour was observed at 4 h, in accordance with the previous studies.[39]

3.6 Organ weight

During the entire study period, no mortality was observed in the treated group after 1, 10 and 100 mg kg^{-1} BW ZnO NPs administered by g.i. and i.p. routes. It is evident that up to 100 mg kg^{-1} ZnO NPs was well tolerated by all the mice groups, implying that the LD_{50} of ZnO NPs is greater than 100 mg kg^{-1} BW. Table 1 displays the BW variation of the mice after g.i. and i.p. administration of ZnO NPs at different concentrations. In the case of g.i. administration, after 1 day, a slightly higher BW is observed except for G-3 whereas after 7 days, the BW regained gradually except for G-1. Again on day 14, a gradual increase in the BW was noticed except for G-3. In the case of i.p. administration, a gradual decrease in BW was noticed except for I-3 after 1 and 7 days, whereas the BW was found to be regained on day 14. During the entire experiment, the ZnO NPs treated for 14

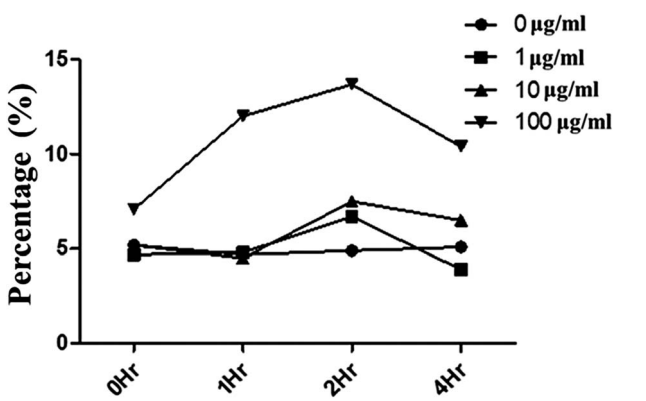

Fig. 5 Graphical representation of the cellular uptake behavior of ZnO NPs. The RAW 264.7 murine macrophages were treated with 1, 10 and 100 μg mL^{-1} FITC–ZnO NPs for 1, 2, 3 and 4 h followed by FACS analysis.

Table 1 Body weight gain of the mice after gastrointestinally (G-1, G-2, G-3) and intraperitoneally (I-1, I-2, I-3) administration with ZnO NPs ($x \pm$ S.D.)[a]

Groups	Before	After 1 day	After 7 days	After 14 days
CT	36.8 ± 2.6	37.0 ± 2.8	37.8 ± 1.8[b]	37.3 ± 2.6
G-1	34.3 ± 1.2	35.0 ± 2.8	32.2 ± 3.4[c]*	36.1 ± 2.4
G-2	33.0 ± 1.7	34.3 ± 1.0	35.8 ± 0.9[b]*	36.7 ± 1.1
G-3	35.8 ± 3.3	33.3 ± 3.0	34.8 ± 2.3[c]*	33.6 ± 2.9
I-1	35.5 ± 1.0	33.6 ± 1.8[c]**	28.0 ± 2.1[c]	36.4 ± 1.8
I-2	35.5 ± 1.6	34.7 ± 0.8[c]**	34.1 ± 1.2[d]	36.2 ± 1.7
I-3	34.0 ± 1.5	34.8 ± 1.3[b]**	35.2 ± 2.1[bd]	36.1 ± 2.9

[a] Results from analysis of covariance (ANOVA) adjusted for the baseline values. [b] The means with the same letter are not significantly different within the same line (Tukey's multiple range test, $\alpha = 0.05$). [*] $P < 0.009$, [**] $P < 0.002$. [c] The means with the same letter are not significantly different within the same line (Tukey's multiple range test, $\alpha = 0.05$). [*] $P < 0.009$, [**] $P < 0.002$. [d] The means with the same letter are not significantly different within the same line (Tukey's multiple range test, $\alpha = 0.05$). [*] $P < 0.009$, [**] $P < 0.002$.

days did not cause any adverse effects on growth as no statistically significant differences in BW gain were observed between the treated and control groups. Furthermore, no behavioural changes and abnormal clinical signs were noticed in either the control or treated groups. Considering all these results together, ZnO NP treatment did not induce any apparent toxicity in male ICR mice although i.p. administration was found to induce a slight decrease in the BW.

The organ weight of mice exposed to different concentrations of ZnO NPs, administered by g.i. and i.p. route to illustrate its influence on organs was presented in Fig. 6. It can be seen that the weights of the heart, lung, kidneys, spleen, liver, and pancreas decreased at 100 mg kg^{-1} BW after g.i. administration. Further, a rise in the weight of the kidney, spleen and pancreas was monitored when intraperitoneally administered. Hence, it is concluded that the weight of kidney, spleen and pancreas strongly varies according to the administration routes, but it was not statistically significant. Organ weight can be a sensitive indicator in toxicology studies. From the fact of organ weight changes, we can suggest that ZnO NPs exert toxic effects against kidney, spleen, and pancreas especially when administered by g.i. route, but it does not exert toxic effects against the same organs when administered by i.p. route. The above findings suggest that the g.i. administration route can affect the g.i. system and damage the immune system. Moreover, this implies that the spleen and pancreas could possibly be one of the target organs for ZnO NPs and may also be involved in their biodistribution and metabolism (in case of g.i. administration).

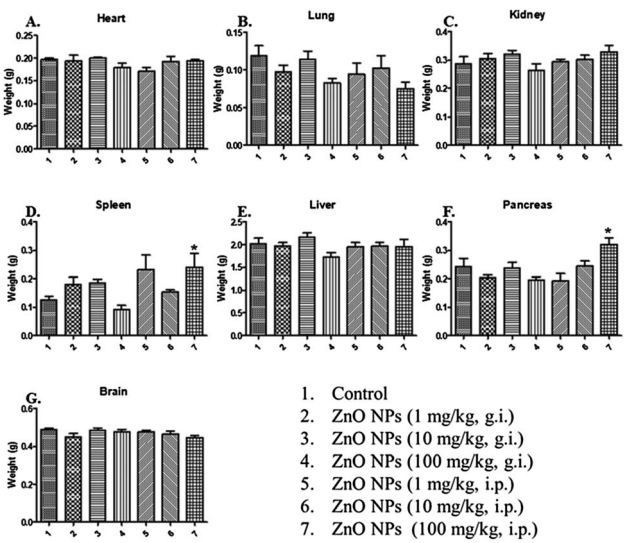

Fig. 6 Organ weight of the mice after exposure to ZnO NPs ($x \pm$ S.D.).

3.7 Serum biochemistry results

Previously, many studies reported that excess oral zinc salt and zinc powder administration can lead to liver damage[40] and liver dysfunction will cause a rise in the levels of the serum enzymes such as ALT/GPT and ALP.[24,41,42] Schliess *et al.* have shown that an increased free intracellular zinc concentration can lead to hepatic encephalopathy which is a neuropsychiatric manifestation of acute and chronic liver failure.[42] Hence, the level of ALT/GPT and ALP was monitored to confirm the proper functioning of the liver. Results demonstrate a significant rise in ALT/GPT and ALP level in the 100 mg kg^{-1} BW treated groups both in the case of g.i. and i.p. administration, suggesting liver dysfunction or damage (shown in Fig. 7 A and B). Cho *et al.* showed that rapid, pH-dependent dissolution of ZnO NPs inside of phagosomes is the main cause of ZnO NPs-induced diverse progressive severe lung injuries.[43] All these reports further confirm that the observed toxicity in the case of our study is basically due to the presence of Zn^{2+} ions as a result of particle dissolution. Likewise, the kidney dysfunction is also characterized by elevated BUN and CRE levels. Therefore, the BUN and CRE levels were evaluated and showed in Fig. 7 (C and D). No remarkable change in the BUN and CRE levels was observed in all the treated groups which symbolizes proper functioning of kidneys in male ICR mice.

3.8 Pathological investigation

Fig. 8 shows the typical histopathological alteration of kidney (A–C), liver (D–F) and lung (G–I) in the mice administered with ZnO NPs for 14 days. The pathological observation in the case of g.i. administration of low ZnO NPs dosage (1 and 10 μg

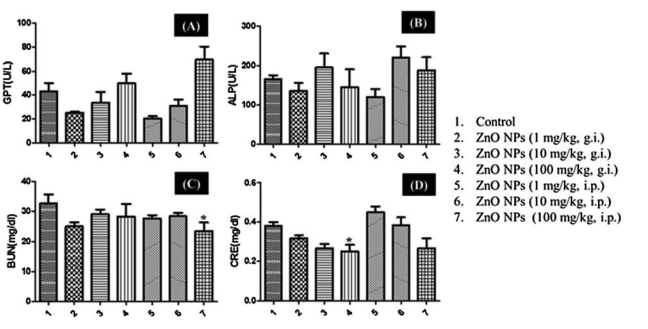

Fig. 7 Biochemical assay of serum in the mice exposed to ZnO NPs for 14 days. (A) GPT. (B) ALP. (C) BUN. (D) CRE.

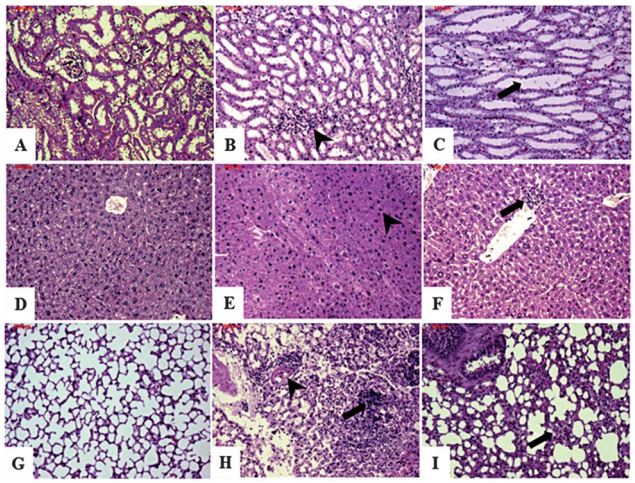

Fig. 8 Histologic changes of the kidney (A–C), liver (D–F) and lung (G–I) after oral treatment of ZnO NPs for 2 weeks. (A) control; (B) ZnO NPs g.i. at 100 μg mL^{-1}; (C) ZnO NPs i.p. at 100 μg mL^{-1}; (D) control; (E) ZnO NPs g.i. at 100 μg mL^{-1}; (F) ZnO NPs i.p. at 100 μg mL^{-1}; (G) control; (H) ZnO NPs g.i. at 100 μg mL^{-1}; (I) ZnO NPs i.p. at 100 μg mL^{-1}. (B) Mild interstitial inflammation (arrow head), (C) focal interstitial edema and inflammation (arrow), (E) early apoptotic change characterized by nuclear pyknosis (arrow head), (F) focal inflammation in the area of central vein, (H) patchy and moderate to severe interstitial inflammation mainly composed of lymphocytes (arrow), destruction of alveolar wall and hyaline membrane (arrow head), (I) moderate interstitial inflammation (arrow).

mL^{-1}) demonstrates mild interstitial and periportal inflammation in kidney and liver (data not shown). Further, an increased ZnO NPs dosage (100 μg mL^{-1}) caused early apoptotic change characterized by mild interstitial inflammation in kidney (B) and nuclear pyknosis in liver (E). Also, patchy and moderate to severe interstitial inflammation mainly composed of lymphocytes, destruction of alveolar wall and hyaline membrane was observed in the lung (H). On the other hand, the case of i.p. administration of low ZnO NPs dosage (1 and 10 μg mL^{-1}) shows early apoptotic change only in liver characterized by nuclear pyknosis (data not shown). At a high ZnO NPs dose (100 μg mL^{-1}) i.p. administered, focal interstitial edema and inflammation in kidney (C), focal inflammation in the central vein area of liver (F) and moderate interstitial inflammation in the lung (I) become prominent. Notably, the pathological damage was found to be provoked by the dose increase in the kidney and liver, which is in accordance with the serum biochemical outcomes. In an overall examination, we noticed white deposits of ZnO NPs in the peritoneal cavity after i.p. administration of 100 μg mL^{-1} ZnO NPs (ESI Fig. S3†). These findings indicate that the ZnO NPs are highly toxic to the lung tissues at higher dosages, which is consistent with previous reports.[44] To our knowledge, this is the first study to report the toxic effects of ZnO NPs through i.p. administration. In summary, ZnO NPs do not produce any appreciable toxicity in *in vitro*, whereas some toxic effects were observed for *in vivo* studies, especially targeting kidneys, lungs and liver. Thus, these studies demonstrate that it is very difficult to draw perfect correlations between *in vitro* and *in vivo* results for evaluating the toxic potential of nanomaterials.

4 Conclusions

In this work, we have systematically investigated the toxicological profile of ZnO NPs in RAW 264.7 murine macrophages (*in vitro*) and male ICR mice (*in vivo*) by using g.i. and i.p. administration routes at different doses. The *in vitro* results showed dose-dependent toxicity of ZnO NPs in RAW 264.7 cells with decreased cell viability, an elevated intracellular ROS level and higher cellular uptake observed at higher NP doses *i.e.* 100 μg mL^{-1}. Compared with the *in vitro* results, the *in vivo* studies showed an obvious dose-dependent trend such as an increment in BW, decreased organ weight and mild to severe pathological inflammation depending on their different administration routes. A rise in the GPT and ALP level was observed which is attributed to liver dysfunction. The results showed that the i.p. administration route was more toxic than the g.i. route as ZnO NPs administered *via* i.p. route induces comparative decrease in BW and severe pathological inflammation in mice. The histopathological results demonstrated that the liver, kidney, lung, spleen and pancreas may be the target organs for ZnO NPs although the statistical significance was not acknowledged. Thus, our results suggest that the toxicity of nanomaterials such as ZnO is closely associated not only with their physiological properties but also varies with selected administration routes. Moreover, as very little correlation was observed between the *in vitro* and *in vivo* studies, it becomes essential to design standard protocols for evaluating the toxic potential of nanomaterials before commercialization.

Acknowledgements

This work was supported in part by the Priority Research Centers Program (2011-0031400) and the World Class University program (R31-20029) funded by the Korean government (MEST). YBH acknowledges the Chonbuk National University for the selection of research-oriented professor in 2012.

Notes and references

1 V. Wagner, A. Dullaart, A. K. Bock and A. Zweck, *Nat. Biotechnol.*, 2006, **24**, 1211.
2 M. Ferrari, *Nat. Rev.*, 2005, **5**, 161.
3 Y.-B. Hahn, R. Ahmad and N. Tripathy, *Chem. Commun.*, 2012, **48**, 10369.
4 R. Ahmad, N. Tripathy, J.-H. Kim and Y.-B. Hahn, *Sens. Actuators, B*, 2012, **174**, 195.
5 R. Ahmad, N. Tripathy and Y.-B. Hahn, *Biosens. Bioelectron.*, 2013, **45**, 281.
6 N. Tripathy, R. Ahmad, H. S. Jeong and Y.-B. Hahn, *Inorg. Chem.*, 2011, **51**, 1104.
7 A. Nel, T. Xia, L. Madler and N. Li, *Science*, 2006, **311**, 622.
8 A. Magrez, S. Kasas, V. Salicio, N. Pasquier, J. W. Seo, M. Celio, S. Catsicas, B. Schwaller and L. Forro, *Nano Lett.*, 2006, **6**, 1121.
9 G. J. Nohynek, J. Lademann, C. Ribaud and M. S. Roberts, *Crit. Rev. Toxicol.*, 2007, **37**, 251.
10 A. Steele, I. Bayer and E. Loth, *Nano Lett.*, 2009, **9**, 501.

11 M. J. Rincker, G. M. Hill, J. E. Link, A. M. Meyer and J. E. Rowntree, *J. Anim. Sci.*, 2005, **83**, 2762.
12 R. Ahmad, N. Tripathy and Y.-B. Hahn, *Sens. Actuators, B*, 2012, **169**, 382.
13 N. Zhang, Z. Chen and Y.-J. Xu, *CrystEngComm*, 2013, **15**, 3022.
14 G. Colon, B. C. Ward and T. J. Webster, *J. Biomed. Mater. Res., Part A*, 2006, **78**, 595.
15 N. Jones, B. Ray, K. T. Ranjit and A. C. Manna, *FEMS Microbiol. Lett.*, 2008, **279**, 71.
16 Y. B. Hahn, *Korean J. Chem. Eng.*, 2011, **28**, 1797.
17 K. Yamaki and S. Yoshino, *BioMetals*, 2009, **22**, 1031.
18 J. W. Rasmussen, E. Martinez, P. Louka and D. G. Wingett, *Expert Opin. Drug Delivery*, 2010, **7**, 1063.
19 Scientific Committee on Cosmetic Products and Non-Food Products (SCCNFP), Evaluation and opinion on: zinc oxide, 24th plenary meeting, Brussels, 2003.
20 T. Xia, M. Kovochich, M. Liong, L. Madler, B. Gilbert, H. Shi, J. I. Yeh, J. I. Zink and A. E. Nel, *ACS Nano*, 2008, **2**, 2121.
21 K. H. Muller, J. Kulkarni, M. Motskin, A. Goode, P. Winship, J. N. Skepper, M. P. Ryan and A. E. Porter, *ACS Nano*, 2010, **4**, 6767.
22 C. Hanley, J. Layne, A. Punnoose, K. M. Reddy, I. Coombs, A. Coombs, K. Feris and D. Wingett, *Nanotechnology*, 2008, **19**, 295103.
23 L. Sophie, R. Francoise, G. Jorina, D. Aurélie, M. M. Emmanuelle, B. Jorge, L. Ghislaine and H. Peter, *Part. Fibre Toxicol.*, 2009, **6**, 14.
24 B. Wang, W. Feng and M. Wang, *J. Nanopart. Res.*, 2008, **10**, 263.
25 C. M. Sayes, K. L. Reed and D. B. Warheit, *Toxicol. Sci.*, 2007, **97**, 163.
26 A. Umar, M. M. Rahman, M. Vaseem and Y.-B. Hahn, *Electrochem. Commun.*, 2009, **11**, 118.
27 Z. Yan, W. Haixia, H. Xuelei, Z. Jingyan and G. Shouwu, *Nanoscale Res. Lett.*, 2011, **6**, 450.
28 J. Casanovas, D. Jacquemin, E. A. Perpete and C. Aleman, *Chem. Phys.*, 2008, **354**, 155.
29 B. J. Zhang, A. Thurber, D. A. Tenne, J. W. Rasmussen, D. Wingett, C. Hanna and A. Punnoose, *Adv. Funct. Mater.*, 2010, **20**, 1.
30 H.-M. Xiong, *J. Mater. Chem.*, 2010, **20**, 4251.
31 H. Wang, D. Wingett, M. H. Engelhard, K. Feris, K. M. Reddy, P. Turner, J. Layne, C. Hanley, J. Bell, D. Tenne, C. Wang and A. Punnoose, *J. Mater. Sci.: Mater. Med.*, 2009, **20**, 11.
32 C. Hanley, A. Thurber, C. Hanna, A. Punnoose, J. Zhang and D. G. Wingett, *Nanoscale Res. Lett.*, 2009, **4**, 1409.
33 T. Xia, M. Kovochich, J. Brant, M. Hotze, J. Sempf, T. Oberley, C. Sioutas, J. I. Yeh, M. R. Wiesner and A. E. Nel, *Nano Lett.*, 2006, **6**, 1794.
34 W. X. Mai and H. Meng, *Integr. Biol.*, 2013, **5**, 19.
35 A. Gojova, B. Guo, R. S. Kota, J. C. Rutledge, I. M. Kennedy and A. I. Barakat, *Environ. Health Perspect.*, 2007, **115**, 403.
36 A. Beyerle, H. Schulz, T. Kissel and T. Stoeger, *J. Phys.: Conf. Ser.*, 2009, **151**, 012034.
37 J. Palomaki, P. Karisola, L. Pylkkanen, K. Savolainen and H. Alenius, *Toxicology*, 2010, **267**, 125.
38 A. Federico, F. Morgillo, C. Tuccillo, F. Ciardiello and C. Loguercio, *Int. J. Cancer*, 2007, **121**, 2381.
39 J. Yu, M. Baek, H. E. Chung and S. J. Choi, *J. Phys.: Conf. Ser.*, 2011, **304**, 012007.
40 B. Wang, W. Y. Feng, T. C. Wang, G. Jia, M. Wang, J. W. Shi, F. Zhang, Y. L. Zhao and Z. F. Chai, *Toxicol. Lett.*, 2006, **161**, 115.
41 J. Kellerman, *Blood Test. Chicago*, Signet Book, USA, 1995.
42 F. Schliess, B. Görg and D. Häussinger, *Metab. Brain Dis.*, 2009, **24**, 119.
43 W. S. Cho, R. Duffin, S. E. Howie, C. J. Scotton, W. A. Wallace and W. Macnee, *Part. Fibre Toxicol.*, 2011, **8**, 27.
44 W. S. Lin, Y. Xu, C. C. Huang, Y. F. Ma, K. B. Shannon, D. R. Chen and Y. W. Huang, *J. Nanopart. Res.*, 2009, **11**, 25.